IEEE Access
Multidisciplinary ⋮ Rapid Review ⋮ Open Access Journal

Received November 19, 2018, accepted December 4, 2018, date of publication December 27, 2018, date of current version January 23, 2019.

Digital Object Identifier 10.1109/ACCESS.2018.2889828

Analysis of Transient Behavior of Mixed High Voltage DC Transmission Line Under Lightning Strikes

MANSOOR ASIF[1], (Student Member, IEEE), HO-YUN LEE[1], (Student Member, IEEE), UMER AMIR KHAN[2], (Member, IEEE), KYU-HOON PARK[1], (Student Member, IEEE), AND BANG-WOOK LEE[3], (Member, IEEE)
[1]HVDC Electric Power Lab, Department of Electrical and Electronic Engineering, Hanyang University, Ansan 15588, South Korea
[2]Department of Electrical Engineering, Capital University of Science & Technology, Islamabad 46000, Pakistan
[3]Division of Electrical Engineering, Hanyang University, Ansan 15588, South Korea

Corresponding author: Bang-Wook Lee (bangwook@hanyang.ac.kr)

This work was supported in part by the Korea Institute of Energy Technology Evaluation and Planning and in part by the Ministry of Trade, Industry and Energy, South Korea, under Grant 20174030201780.

ABSTRACT Growing urbanization coupled with increased power demands have led to increasing use of mixed power transmission lines with sections of overhead lines (OHL) and underground cables. Due to differences in surge impedance of cables and OHL, voltage surges experience reflections and refractions at their boundaries which make the transient behavior of mixed high voltage direct current (HVDC) line quite peculiar. Lightning strikes on overhead sections of lines induce voltage surges that travel along OHL and enter the cable section. Lightning overvoltage can cause OHL insulators to flashover and stress cable insulation or cause its permanent breakdown. In this paper, we simulated a fast front model of a mixed HVDC transmission line using an electromagnetic transient simulation program (PSCAD) to analyze its transient behavior under a lightning strike. The leader progression model has been used to predict the dielectric performance of OHL insulators. It has been shown that transition towers adjacent to the cable section are much less vulnerable to flashover than subsequent towers. The length of a riser section (connecting OHL and cable) and tower footing impedance have shown to significantly influence the flashover performance of OHL insulators. In addition, the length of cable segments and sheath grounding impedance has been found to influence cable overvoltage. This paper can be used to evaluate the insulation coordination and overvoltage protection requirements for a mixed HVDC transmission line.

INDEX TERMS DC cable, dielectric breakdown, HVDC transmission, insulation coordination, insulator flashover, lightning overvoltage, negative lightning strokes, parametric analysis, *PSCAD/EMTDC*, sheath grounding.

I. INTRODUCTION

Commercial application of high voltage direct current (HVDC) transmission has seen a tremendous rate of increase since the commission of the first HVDC transmission project over five decades ago. The very first applications of HVDC were mainly an interconnection of islands or an interconnection of offshore energy sources, where ac transmission was prohibitively inefficient [1], [2]. Advances in semiconductor and conversion technologies made HVDC transmission commercially attractive for terrestrial power interconnections over long distances. It has since been readily adopted by countries with large inhabited geographical boundaries like the United States, Canada, China, and India.

Cable sections in transmission lines are sometime unavoidable due to the unavailability of overhead right of way in urban areas, river crossings, and the interconnection of offshore energy resources. Due to differences in characteristic impedance of overhead lines (OHL) and cables, a lightning surge traveling from an OHL to a cable is partly refracted into the cable, whereas the rest of it is reflected into the OHL and results in a unique voltage stress on the insulation of the OHL. The part of voltage surge refracted into cable experiences

 This work is licensed under a Creative Commons Attribution 3.0 License. For more information, see http://creativecommons.org/licenses/by/3.0/

repeated reflections inside cable at OHL-cable boundaries and results in a rapid build-up of voltage inside the cable [3].

Insulation of mixed HVDC transmission lines can experience overvoltage stress due to lightning strikes on overhead ground wires (OHGWs) or overhead power conductors (OHPCs).

OHGWs shield power carrying conductors from direct lightning strikes. High magnitude lightning strikes, up-to 200 kA, are attracted by OHGWs and result in a build-up of voltage on towers and stress the OHL insulation. In extreme cases, it can cause flashover of insulators or airgaps. If the sheath of the cable is being used as an earth continuity conductor, these lightning strikes can also result in cable overvoltage [15].

However, lightning strokes with smaller current magnitudes (below shielding current level), generally up-to 20 kA, can bypass the OHGWs and directly strike OHPCs [5]. The voltage surge induced by lightning strikes on OHPCs can cause insulator flashover which appears as a ground fault. This voltage surge can also enter the cable and cause stress to its insulation. As opposed to self-recovering insulation of OHL, extreme overvoltage stress can cause permanent failure of cable insulation [7], [8].

Therefore, it is important to understand the transient behaviour of mixed HVDC transmission lines under lightning strikes so that appropriate insulation coordination and overvoltage protection strategy can be adopted.

In summary, we have made the following contributions through this paper,

- Identified the difference in flashover performance of insulators of the transition tower and subsequent towers.
- Explained the reason for superior flashover performance of transition tower insulators.
- Analysed the influence of the riser section (connecting OHL and cable) on flashover performance of OHL insulators.
- Analysed the influence of tower footing impedance on flashover performance of OHL insulators.
- Analysed the influence of sheath grounding distance and sheath grounding impedance on cable overvoltage.

In the following sections, we have summarized the related studies, explained models of system components, and presented simulation results and their analysis.

II. RELATED STUDIES & LITERATURE GAP

Lightning strikes on overhead HVDC transmission lines can result in insulation failure i.e., back flashover; however, insulators of overhead lines are self-recovering. On the other hand, cables in station-to-station dc cable transmission systems without any section of OHL terminating inside dc valve halls, never have to face the lightning strikes [28]. However, lightning strikes on overhead sections in mixed transmission lines can result in overvoltage in the cable and lead to permanent failure of the cable insulation [29]. Therefore, the behaviour of lightning transient in mixed transmission lines has been the subject of interest since the 1990s. Mixed dc transmission lines have been studied in [3], [12], and [27] whereas [4], [6], [9], [10], [11], [26] covered mixed ac transmission lines.

A comprehensive analysis of lightning overvoltage in dc cable crossing under the St-Lawrence River was presented in [3]. A 4-km long cable is a part of a 1500 km, 500 kV bipolar dc transmission line. Coaxial overvoltage in cable caused by lightning strikes on the OHPCs and OHGWs were studied. Lightning overvoltage analysis of a ±525 kV mixed dc line with surge arresters installed on the cable terminal was presented in [12]. A lightning overvoltage study of a 380-kV, 50 Hz mixed line considering lightning strikes on the transition tower was presented in [9]. The effect of sheath's "bonding lead inductance" and "surge voltage limiter" on lightning overvoltage was presented in detail. In [10], results of [9] were verified and in addition, an overvoltage study was performed on the cable with shunt reactors installed on terminals. A lightning overvoltage study in a 380-kV, 50 Hz transmission line composed of 4 cable sections of varying lengths in a OHL-cable-OHL configuration in the Netherlands was performed in [11]. Lightning overvoltage in cable sections with and without the presence of surge arresters was analysed and compared. The impact of OHL geometries and footing impedance on maximum overvoltage along a section of dc extruded cable was analysed in the presence of surge arresters at cable terminals in [27]. The effect of a frequency dependent footing impedance model was analysed and compared with fixed impedance models in [26]. Reference [4] also analysed the effect of current dependent footing resistance in addition to corona on lightning overvoltage. It was found that constant tower footing impedance results in higher overvoltage compared to dynamic frequency dependent impedance models [4], [26].

References [3], [9], [10] considered lightning strikes near transition towers to produce extreme overvoltage stress which has been contradicted by [4] and [12]. Reference [3] describes the back-flashover on transition towers to produce maximum overvoltage, however [4] and [12] rule out the possibility of back-flashover on transition towers. Reference [4], describes the reason for a seemingly lower insulation strength of subsequent towers as reflected waves from neighbouring towers arriving at same time and superposing to cause insulator flashover. This has been found to be an insufficient explanation, especially for cases of flashover resulting from shielding failure. In such cases, no reflections have been observed from neighbouring towers.

In [3], the length of riser section is more than twice of the tower height, whereas [9] has used an unspecified length. The direct connection of cable with OHL at transition towers have been considered in [4], [11]–[13], [26], and [27]. In this paper the length of the riser section has shown to have a significant influence on the flashover performance of OHL insulators.

References [3], [12], [27] did not use the sheath as an earth continuity medium. In [3], the sheath of the HVDC cable was grounded only at terminals. Reference [12] considered a solidly grounded sheath with variable sheath grounding

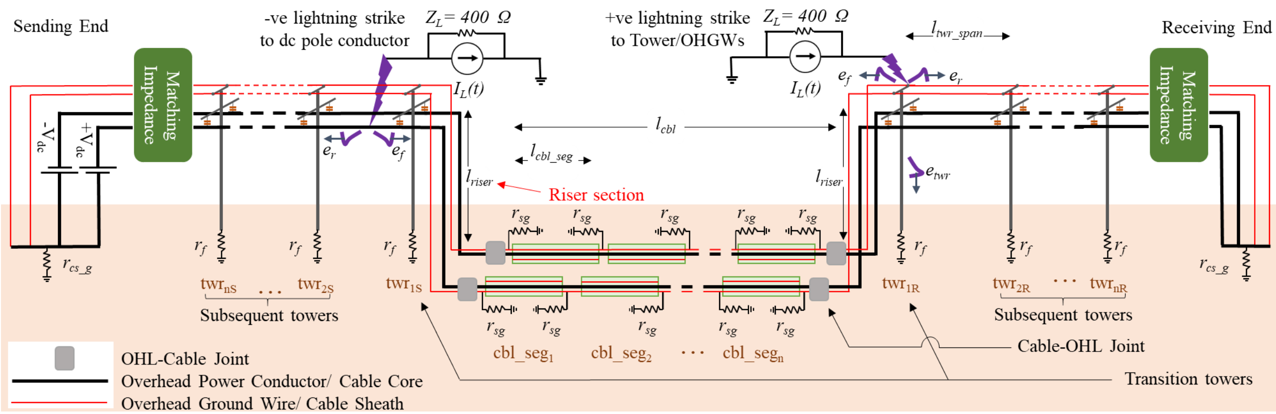

FIGURE 1. Model of lightning transient analysis in a mixed HVDC transmission line. A small cable section is present between two overhead line sections terminating in matching impedance to avoid reflection of voltage surge from remote ends of the transmission line.

distances to measure the sheath-ground overvoltage at the cable entrance. In reference [27], the sheath was grounded every 2.5 km with a fixed grounding impedance. Sheath grounding of HVDC cable systems considering lightning transient phenomenon has been recognized as an important topic for further research [12], [24], [25], [27].

III. SYSTEM DESCRIPTION & MODELLING CHOICES

In this paper a bipolar ± 500 kV dc transmission line is composed of a cable section between two OHL sections as shown in Fig.1. Five towers on both sides of cable are accurately modelled to consider the effect of reflections from the tower structure on the overvoltage magnitude. OHL sections beyond the towers are represented by matching impedance at both sending and receiving ends. Matching impedances present equivalence of an infinite line and prevent the lightning voltage wave e_r, from reflecting at the terminals.

A finite length cable is used with a length up to 25 km. The sheath of the cable is used as an earth continuity conductor i.e. solidly bonded to OHGWs. Sheath grounding impedance is represented by a constant resistance r_{sg}. To verify the effect of sheath grounding distance and impedance on the magnitude of the sheath-ground overvoltage, the number and length of cable segments is kept as a variable with the sheath of each segment grounded at its terminals.

EMT models of system components are developed as per guidelines given in [5] and [21]. The component models are described in the following subsections.

A. TOWER MODEL

To accurately represent the overvoltage across insulators, the vertical section of tower is divided into two sub-sections connected at cross arms as shown in Fig. 2.

Multistorey tower models in [14]–[16] have been shown to yield inadequate results when used to model shorter low voltage towers [30]. Owing to the relatively small height of HVDC tower, it is represented by a single conductor frequency independent distributed parameter line with the same surge impedance for upper and lower sections [31], [32].

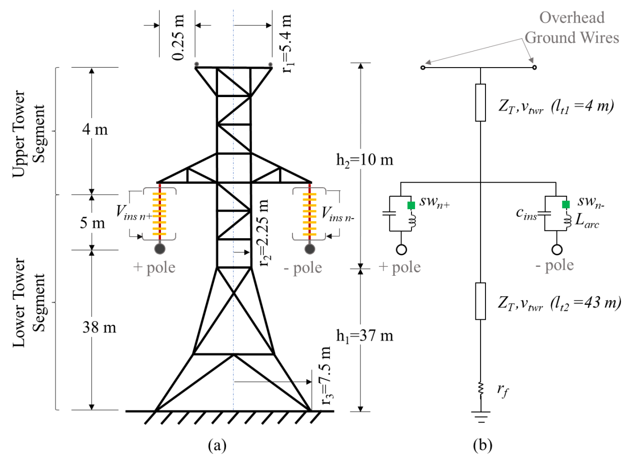

FIGURE 2. Overhead section of the bipolar HVDC transmission line. (a) tower structure (not drawn to scale). (b) circuit model for electromagnetic transient simulation.

The wave propagation on the tower is retarded by cross arms and braces. Therefore, the velocity of the traveling wave on the tower is assumed to be 85% of the speed of light [33]. The approximate surge impedance of the waisted tower structure, as shown in Fig. 2, is calculated using (1) [34].

$$Z_T = 60\, ln \left\{ \cot \left(\frac{1}{2} tan^{-1} T \right) \right\} \tag{1}$$

where,

T: Intermediate value → $\{r_1 h_2 + r_2(h_1 + h_2) + r_3 h_1\}/(h_1 + h_2)^2$

h_1: height from base to waist

h_2: height from waist to top

r_1: tower radius at top

r_2: tower radius at waist

r_3: tower radius at base

B. TOWER FOOTING IMPEDANCE

A prudent model of tower footing impedance is very important to conservatively estimate the values of overvoltage magnitude at the tower top and the overvoltage stress on OHL as well as the cable insulation. The impedance of high resistivity soil is known to be strongly dependent on frequency [35], [36].

However, models considering frequency dependence have shown optimistic estimates of lightning overvoltage [26]. Because the impedance of frequency dependent models recommended in [5], [35], and [36] decreases during a lightning surge, this results in an increased magnitude of opposite polarity reflected surge from the base of the tower. Therefore, the peak overvoltage level at the tower top or across OHL insulators is generally decreased.

The degree of frequency dependency of soil varies with its resistivity which varies over time and depends on weather conditions. In addition, it is very hard to determine the actual conditions of the soil. Therefore, to obtain conservative estimates of overvoltage, the footing impedance is represented by a constant resistance r_f as recommended by [14], [15], and [26].

C. INSULATORS

Insulators strings are composed of 29 disks of cap and pin suspension ceramic insulators with a 5 m air gap between arc horns as shown in Fig. 2. The capacitance of one insulator disk is approx. 80 pF [5].

The Leader Progression Model (LPM) is used for predicting flashover of an insulator. The LPM determines the time taken to breakdown by considering the physical discharge process according to the gap configuration [21]. The total time taken to breakdown, t_c is given by (2)

$$t_c = t_i + t_s + t_l \tag{2}$$

where,

t_i: Corona inception time, μs

t_s: Streamer propagation time, μs

t_l: Leader propagation time, μs

The corona inception voltage is much smaller than the breakdown voltage, and due to the rapid rate of increase of voltage, the corona inception time t_i is negligible, and is usually assumed to be zero. If the voltage continues to increase after the corona inception, a streamer begins to grow and cross the gap after time t_s (3),

$$\frac{1}{t_s} = 1.25\left(\frac{E}{E_{50}}\right) - 0.95 \tag{3}$$

where,

E: Maximum gradient in the gap before breakdown, kV/m

E_{50}: Average gradient at the critical flashover (CFO) voltage, kV/m

After t_s a leader starts to develop, with an exponentially increasing velocity given by (4),

$$\frac{dL}{dt} = KV(t)\left[\frac{V(t)}{g-L} - E_0\right] \tag{4}$$

where,

$V(t)$: Voltage across gap, kV

L: Leader length, m

g: Gap Length, m

K: Leader Coefficient, $m^2/kV^2.s$

E_0: Critical Leader inception gradient, kV/m

K and E_0 for cap and pin type suspension insulators under negative polarity stress are given in Table. 1. Leader length L becomes equal to the gap length g after time t_l and breakdown occurs.

TABLE 1. Values of EMT simulation model parameters.

Symbol	Quantity	Value
h	height of tower	47 m
l_{t1}	Length of upper tower segment	4 m
l_{t2}	Length of lower tower segment	43 m
Z_T	Charac. impedance of tower segments	139 Ω
r_f	Footing impedance	10 Ω
r_{sg}	Sheath-grounding impedance	10 Ω
c_{ins}	Capacitance of insulator	2.75 pF
L_{arc}	Insulator arc inductance	5 µH
l_{twr_span}	Length of tower span	350 m
Z_{OHPC}	Characteristic Impedance of OHPC	465.3 Ω
Z_{OHGW}	Characteristic Impedance of OHGW	541.8 Ω
Z_{core}	Characteristic Impedance of cable core	72.7 Ω
Z_{sheath}	Characteristic Impedance of cable sheath	27.1 Ω
v_{OHGW}	wave velocity on OHGW	2.8 E8 m/s
v_{OHPC}	wave velocity on OHPC	2.8 E8 m/s
v_{core}	wave velocity on cable core	6.4 E7 m/s
v_{sheath}	wave velocity on cable sheath	2.7 E7 m/s
v_{twr}	wave velocity on tower segments	2.55 E8 m/s
l_{riser}	length of riser section	50 m
y	time of lightning strike	0.007 s
K	Leader coefficient	1.3 $m^2/kV^2.s$
E_0	Critical Leader Inception Gradient	600 kV/m

In the PSCAD simulation, the insulator breakdown is represented by a switch connected in parallel with an equivalent insulation capacitance c_{ins}, as shown in Fig. 2. The inductive nature of the arc path is taken into consideration by inserting an inductance L_{arc} in series with the switch, according to the recommendation of [37].

D. TRANSMISSION LINE

The choice of the cable and overhead conductor is made to ensure of a power rating of 660 MW per pole of the HVDC line. Sections of the bipolar overhead line, including the OHGWs, are modelled according to geometry shown in Fig. 2. Midspan conductor sag is 10 m for all conductors. OHPCs are modelled based on *Parrot ACSR 54/19*, whereas 1/2 *high strength steel* is used to model the OHGWs.

The 500 kV (2100 mm^2) underground cables based on [18] are arranged in a horizontal configuration as shown in Fig. 3.

The overhead line, as well as underground cables, are modelled using the Universal Line Model (ULM) which considers the frequency dependence of the transformation matrix [38]. *PSCAD* implementation of the ULM called the *frequency dependent (phase) model* has been used and is explained in [39].

Reference [3] used the J. Marti model, whereas [9] has employed an uncoupled transmission line for the riser section modelling. Currently, no guideline is available for modelling

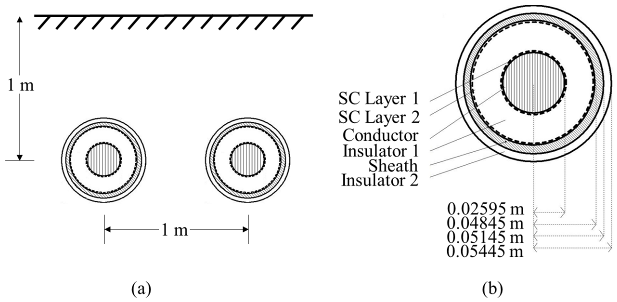

FIGURE 3. Underground section of the bipolar HVDC transmission line (a) cable layout (b) cable structure and dimensions.

of the riser section. Therefore, we have employed the ULM and conductor geometry similar to OHGW/OHPC to model the riser section.

Characteristic impedance and wave velocity of overhead and cable conductors are calculated using the *PSCAD* line constant program (LCP) and are listed in Table. 1. The characteristic impedance and wave velocity of grounding and power carrying riser sections are the same for OHGW and OHPC respectively.

E. LIGHTNING STROKE

Lightning stroke is modeled using the current source in parallel with the resistance that represents the impedance of the lightning channel as shown in Fig. 1. Resistance of 400 Ω has been widely accepted to be a suitable estimate for the impedance of lightning channel [19].

Representative lightning current wave-shapes i.e. ramped, double exponential, and concave are alternatingly used in literature. However, they tend to produce overvoltages with significantly different peak values and time to crest [20].

An upwardly concave lightning current waveform, shown in Fig. 4, is closest to the actual recorded lightning current wave-shapes given in [21] and [40]. It can be mathematically represented by (5),

$$i(t) = \begin{cases} At + Bt^n, & t < t_n \\ I_1 e^{-\frac{(t-t_n)}{t_1}} - I_2 e^{-\frac{(t-t_n)}{t_2}}, & t > t_n \end{cases} \tag{5}$$

The wave shape constants A, B, t_n, n, I_1, I_2, t_1 & t_2 are listed in Table 2, and are derived as per the procedure described in [21].

TABLE 2. Parameters of lightning current impulse.

	Parameters of Strike	OHPC Strike	Tower/OHGW Strike
I_p	peak current	20 kA	200 kA
t_{30}	front (30% - 90%)	3 μs	8 μs
t_f	Effective front time	5 μs	13.33 μs
t_t	tail time	77.5 μs	200 μs
S_m	maximum steepness	20 kA/μs	48 kA/μs
n	wave-shape constant	18.6	11.171
A	//	1.061 kA/μs	4.325 kA/μs
B	//	3.257E-17 kA/μs	9.247 E-14 kA/μs
t_n	//	8.653 μs	21.858 μs
t_1	//	99.324 μs	257.004 μs
t_2	//	0.1 μs	0.416 μs
I_1	//	20.020 kA	200.324 kA
I_2	//	2.0201 kA	20.324 kA

The cumulative probability of a lightning stroke current exceeding 200 kA is 0.77 % [40]. Therefore, we choose 200 kA as the peak magnitude of the lightning stroke terminating at the tower top or OHGWs, which has also been recommended by the IEEE modelling guideline [5].

Shielding failure analysis is performed to compute the peak lightning current that can terminate on OHPCs. Several models have been proposed for shielding failure analysis of the overhead transmission lines. Amongst them the electro-geometric model (EGM) proposed by IEEE Std 1243:1997 has been shown to yield a relatively high maximum shielding failure current (I_{MSF}) [41]. Therefore, to account for the worst-case scenario, the EGM proposed by IEEE Std. is applied on the geometric model shown in Fig. 5.

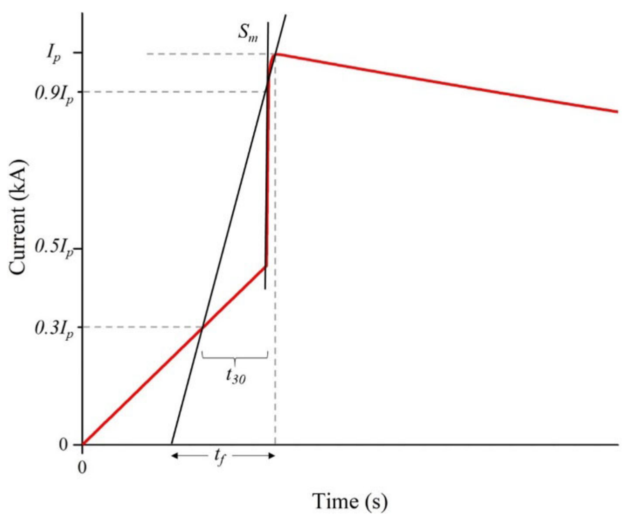

FIGURE 4. Concave front lightning wave-shape recommended by CIGRE for analysis of lightning transients [21].

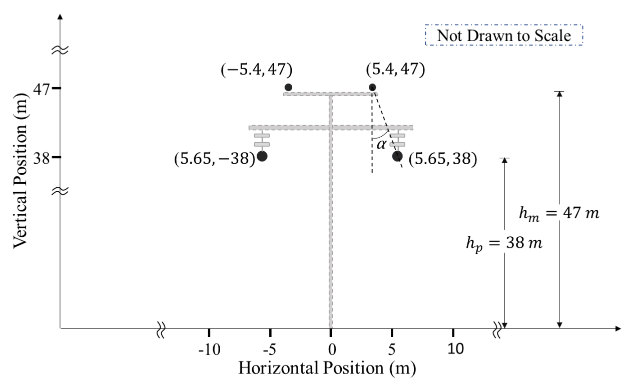

FIGURE 5. Geometric Model of the Tower Structure for determination of maximum shielding failure current (I_{MSF}).

The I_{MSF} is calculated using (6) is 20 kA,

$$I_{MSF} = \left[\frac{\gamma(h_m + h_p)/2}{A(1 - \gamma sin\alpha)}\right]^{1/B} \tag{6}$$

where,
h_m: height of OHGWs
h_p: height of OHPCs
Factors of EGM recommended by IEEE Std.: A, B, γ
γ: $1/\beta$ *where* $\{\beta = 0.36 + 0.17ln(43 - h_p) \Rightarrow h_p \leq 40\text{ m}\}$
α: Shielding angle

The median front times and maximum steepness corresponding to the peak magnitude of a lightning impulse are used as recommended in [5]. Due to the relatively smaller cable and riser sections, the tail time is expected to have influence on the insulation performance of the line; therefore, it is chosen conservatively as per recommendation of [21]. Parameters of the lightning impulse wave-shape are listed in Table 2.

IV. RESULTS & DISCUSSION

As discussed earlier lightning can strike the OHPCs or the OHGWs and the tower top. In the following section results of simulation study for the two types of lightning strikes is presented and analysed in depth.

A. STRIKE ON OVERHEAD POWER CONDUCTOR

Negative polarity lightning strikes on negative pole conductors will produce the highest overvoltage stress on the cable as well as OHL insulators. Therefore, only such lightning strikes are considered in this study.

A negative lightning strike on the negative OHPC is shown in Fig. 1. This lightning strike will initiate a voltage surge e_f traveling on OHPC in forward direction towards the cable and e_r in reverse directions towards the dc source. The equivalent circuit is represented in Fig. 6. OHPCs are connected to towers via insulators which are represented by switches sw_{1-} & sw_{2-} as shown in Fig. 6. When the forward traveling wave e_{f1} arrives at boundary a, part of it is refracted inside the cable core and the rest is reflected into the OHPC. Part of the wave e_{f2} is refracted inside the cable and also experiences reflection and refraction at boundary b. According to the traveling wave theory, the magnitude of the refracted and reflected portions of the wave at the boundaries can be given by (7), (8), and (9).

$$e_{f2} = e_{f1}\frac{2 * Z_{core}}{Z_{OHPC} + Z_{core}} \tag{7}$$

$$e_{r1} = e_{f1}\frac{Z_{core} - Z_{OHPC}}{Z_{OHPC} + Z_{core}} \tag{8}$$

$$e_{r2} = e_{f2}\frac{Z_{OHPC} - Z_{core}}{Z_{OHPC} + Z_{core}} \tag{9}$$

Refracted wave e_{f2} will have the same polarity as the incident wave e_{f1}. However, since the characteristic impedance of the cable core is much lower than the OHPC/riser, the reflected wave e_{r1} at boundary *a* will have the opposite polarity compared to the incident wave and its magnitude will be about 73% of e_{f1}. On the other hand, the reflected wave e_{r2} at boundary *b*, will have the same polarity as the incident wave and its magnitude will also be 73% of the incident wave e_{f2}.

Simulation results for lightning strikes on the transition tower, subsequent towers, and their comparison are presented in the following subsections.

1) AT THE TRANSITION TOWER

As shown in Fig. 6, negative polarity lightning strikes the negative pole OHPC at twr_{1S}. The tower is electrically isolated from the OHPC by an insulator, represented by an open switch in the EMT simulation. Overvoltage at cable entrance (boundary *a* in Fig. 6) as a function of cable length

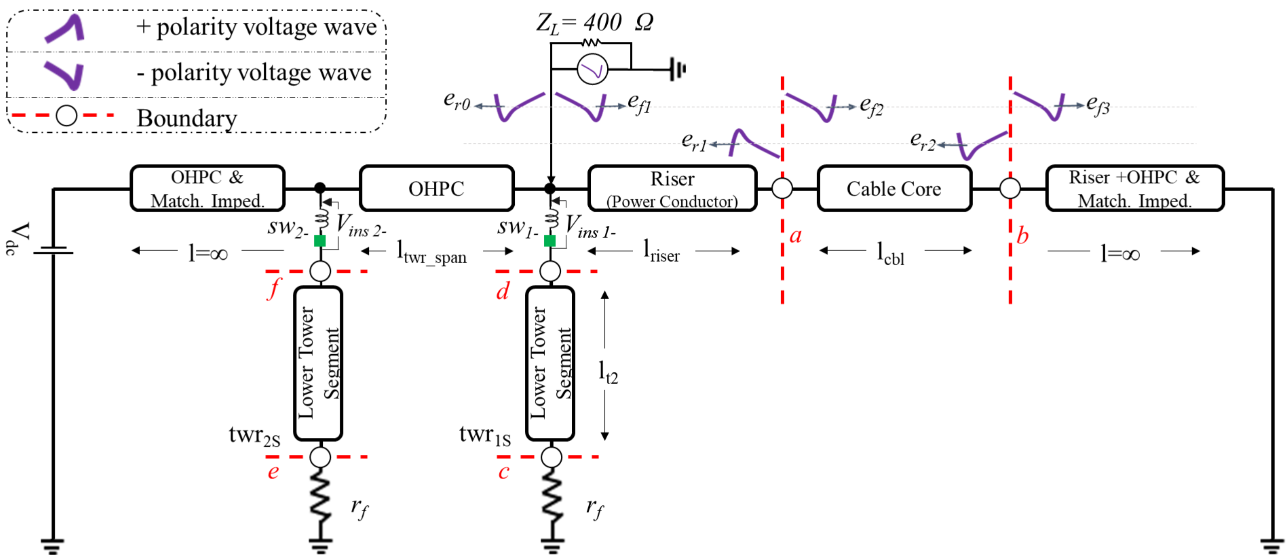

FIGURE 6. Equivalent circuit of a mixed dc transmission line for analysis of lightning strikes on negative pole conductors (only two towers closest to the sending end of cable are considered in this equivalent circuit).

is shown in Fig. 7. In the longer cable sections (25 km), reflected wave e_{r2} will arrive at cable entrance after sufficient attenuation of the incident wave e_{f2}. However, in smaller cables (12.5 km, 6.25 km or 3.125 km) the arrival of reflected wave e_{r2} at cable entrance results in an increase of the peak overvoltage.

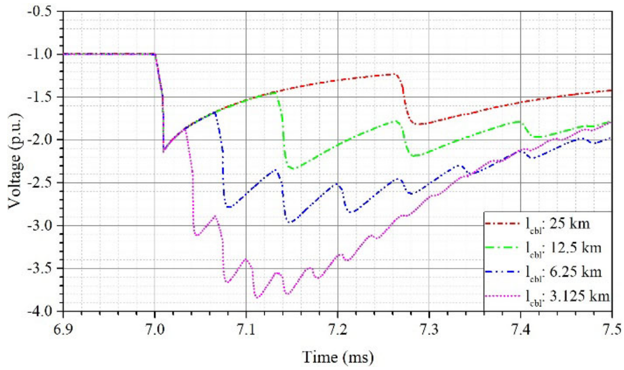

FIGURE 7. **Voltage at entrance (boundary a) of negative pole cable. Lightning strikes a negative OHPC at sending end transition tower (*twr_{1S}*).**

The results indicate that, flashover of OHL insulation did not take place regardless of the cable length.

2) AT SUBSEQUENT TOWERS

Voltage at the cable entrance for various cable lengths is shown in Fig. 8. Insulator flashover occurs regardless of the cable length.

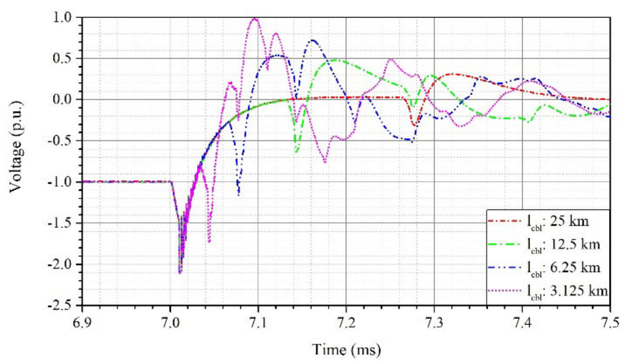

FIGURE 8. **Voltage at entrance (boundary *a*) of a negative pole cable. Lightning strikes a negative OHPC at sending end subsequent tower (*twr_{2S}*) and causes flashover.**

After the flashover of twr_{2S} insulator, i.e. closure of sw_{2-} (in Fig. 6), a part of lightning voltage surge travels towards the ground through the tower. An opposite polarity voltage wave is reflected from the tower base at boundary *e* because the footing impedance of the tower is much lower than its characteristic impedance. The reflected wave will arrive at the top of the tower segment i.e. boundary *f*, where part of it will be refracted into the OHPC towards the cable and part towards the dc source. This positive polarity voltage surge will be repeatedly reflected inside the cable. Due to lower attenuation and travel time in smaller cables, the repeated reflections will result in a higher voltage dip.

3) DIFFERENT INSULATION STRENGTHS

As it is evident from above results, insulators of subsequent towers are prone to flashover, whereas the insulator of the transition tower does not experience flashover from lightning strike on pole conductors.

To understand this phenomenon, insulator voltages and the growth of their respective leader for lightning strikes on the transition (twr_{1S}) and subsequent (twr_{2S}) towers are shown in Fig. 9 and Fig. 10, respectively.

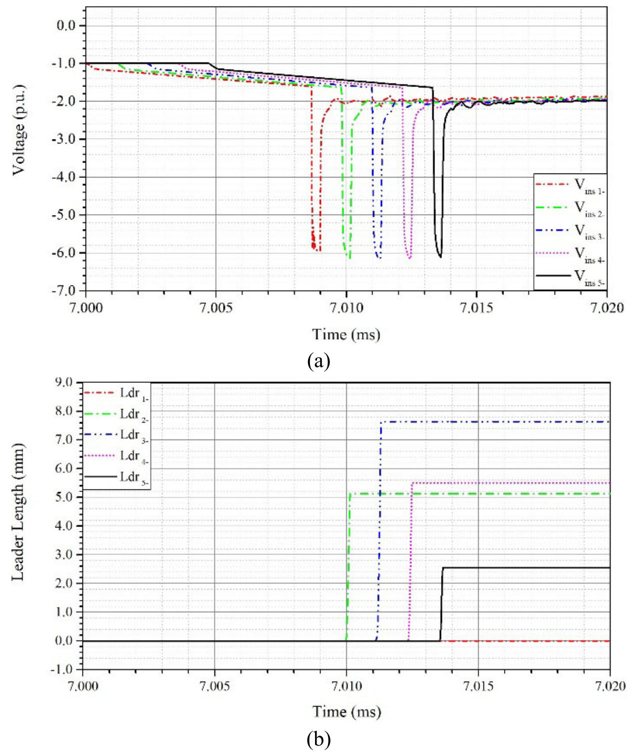

FIGURE 9. **Lightning strikes the negative OHPC at sending end transition tower (twr_{1S}). (a) voltage across the negative pole insulators. (b) Leader growth between insulator arc horns.**

The case of a LIGHTNING STRIKE on a negative OHPC at twr_{1S} is shown in Fig. 6. The location of the strike is separated from the cable by a 50 m long riser section. The voltage surge e_{f1} induced by lightning will travel towards the cable. A part of this forward traveling voltage surge, i.e., e_{f2}, will enter the cable, whereas rest of it, i.e., e_{r1}, will be reflected towards the tower. The reflected wave e_{r1} will arrive at the location of the strike 0.357 μs after the inital strike (at 7.000357 ms) and attenuate the voltage slope, as shown in Fig. 9(a). Under the influence of increasing e_{f1} and proportionally increasing opposite polarity e_{r1}, the voltage across the insulator will continue to grow slowly until the arrival of the steepest portion of the lightning wave at 7.008643 ms. However, a proportional opposite polarity e_{r1} will attenuate it at 7.009 ms (i.e., after 0.357 μs). Due to the relatively small time taken by the reverse traveling wave to arrive at

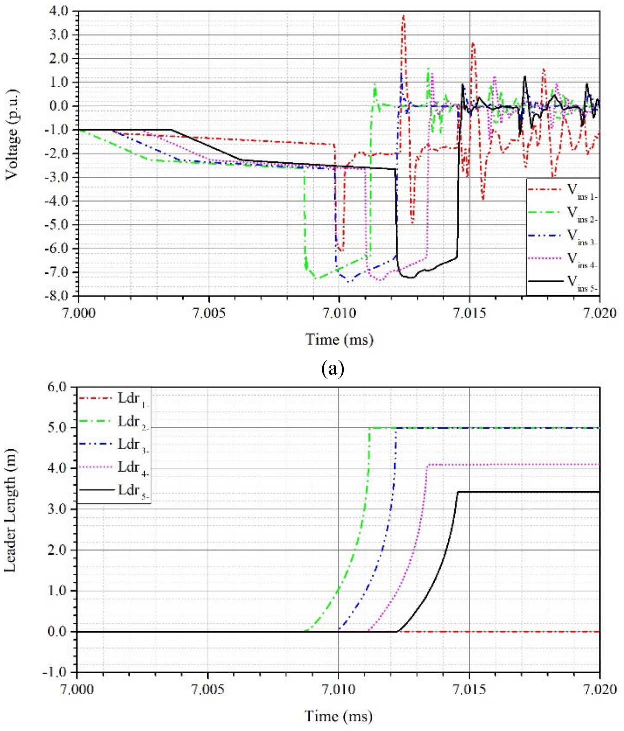

FIGURE 10. Lightning strikes the negative OHPC at sending end subsequent tower (twr_{2S}). (a) voltage across negative pole insulators. (b) Leader growth between insulator arc horns.

the location of strike, the leader of negative pole insulator of twr_{1S} will not grow, as shown in Fig. 9(b).

twr_{2S}, twr_{3S}, twr_{4S}& twr_{5S} are separated from the location of lightning strike by 350 m, 700 m, 1050 m and, 1400 m, respectively. Part of the negative polarity lightning voltage surge (i.e., e_{r0}) traveling toward the dc source, arrives at these tower locations after 1.25 μs, 2.5 μs, 3.75 μs, and 5 μs, respectively. Whereas the positive polarity reflected wave (i.e., e_{r1}) arrives at these tower locations after 1.607 μs, 2.857 μs, 4.107 μs, and 5.357 μs, respectively, i.e. 0.357 μs after the arrival of e_{r0}. Since the reflected wave e_{r1} will be attenuated by the time it arrives at the farther tower locations, the voltage across insulators of these towers will grow further, and initiate leader growth as shown in the fig. 9(b). however, due to the attenuation of both the negative polarity incident wave e_{r0} and the positive polarity reflected wave e_{r1}, the leader growth at the farthest towers i.e., twr_{4S} & twr_{5S} will be relatively lower.

In the case of lightning strike on negative OHPC at twr_{2S}, the negative pole insulator of the transition tower will not experience leader growth, whereas insulators of the remaining towers will experience very high voltage buildup and leader growth, as shown in Fig. 10. twr_{1S} is 350 m from the location of the strike. The negative polarity forward traveling wave will arrive at twr_{1S} after 1.25 μs whereas the positive polarity reflected wave will arrive after 1.607 μs i.e., 0.357 μs after the arrival of the incident wave. This reflected wave results in attenuation of the incident voltage wave at twr_{1S}, as shown in Fig. 10 (a). However, the incident voltage surge will arrive at twr_{2S}, twr_{3S}, twr_{4S}, and twr_{5S} after 0 μs, 1.25 μs, 2.5 μs, and 3.75 μs, respectively. Whereas the positive polarity voltage surge reflected from the cable at boundary *A* will arrive at these tower locations after 2.857 μs, 4.107 μs, 5.357 μs, and 6.607 μs, respectively. The arrival of the positive polarity reflected voltage surge at all subsequent tower locations will be delayed by 2.857 μs compared to the incident wave. This can be seen in Fig. 10 (a), where the attenuation of voltage across negative pole insulators of subsequent towers takes place 2.857 Îijs after the sudden increase in voltage. The leader crosses the arc horn gap and flashover occurs at the insulator of twr_{2S} and twr_{3S}. By the time the incident wave arrives at twr_{4S} & twr_{5S} it is attenuated and is not able to cause sufficient leader growth to result in insulator flashover.

It can be seen in Fig. 11 that if the length of riser section is increased sufficiently the flashover of the transition tower insulator is possible. This result can be attributed to the fact that if the riser section is longer, the opposite polarity reflected wave will require longer to arrive at twr_{1S} and allow the buildup of voltage of the incident wave to a high enough level to cause flashover.

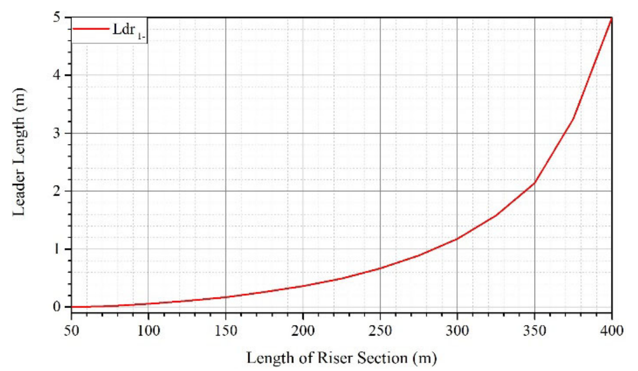

FIGURE 11. Lightning strikes the negative OHPC at sending end transition tower (twr_{1S}). The leader growth and possibility of flashover increases with increasing length of riser section (in Fig. 1).

B. STRIKE ON OVERHEAD GROUND WIRE

A lightning strike on the OHGWs results in part of the lightning surge travelling along OHGWs in both the forward and reverse directions, whereas the rest of it travels along tower as shown in Fig. 12.

When the forward traveling wave arrives at boundary *a*, a part of it is refracted inside the cable sheath and rest is reflected into the riser section towards the OHGWs. The part of the wave e_{f2} refracted inside the cable also experiences reflection and refraction at boundary *b*. Part of the voltage surge e_{d1} that travels down the tower segment is reflected at boundary *c*, whereas the rest of it is absorbed by the ground. Note, that the downward travelling wave will be negative polarity, whereas the upward traveling reflected wave will be positive polarity.

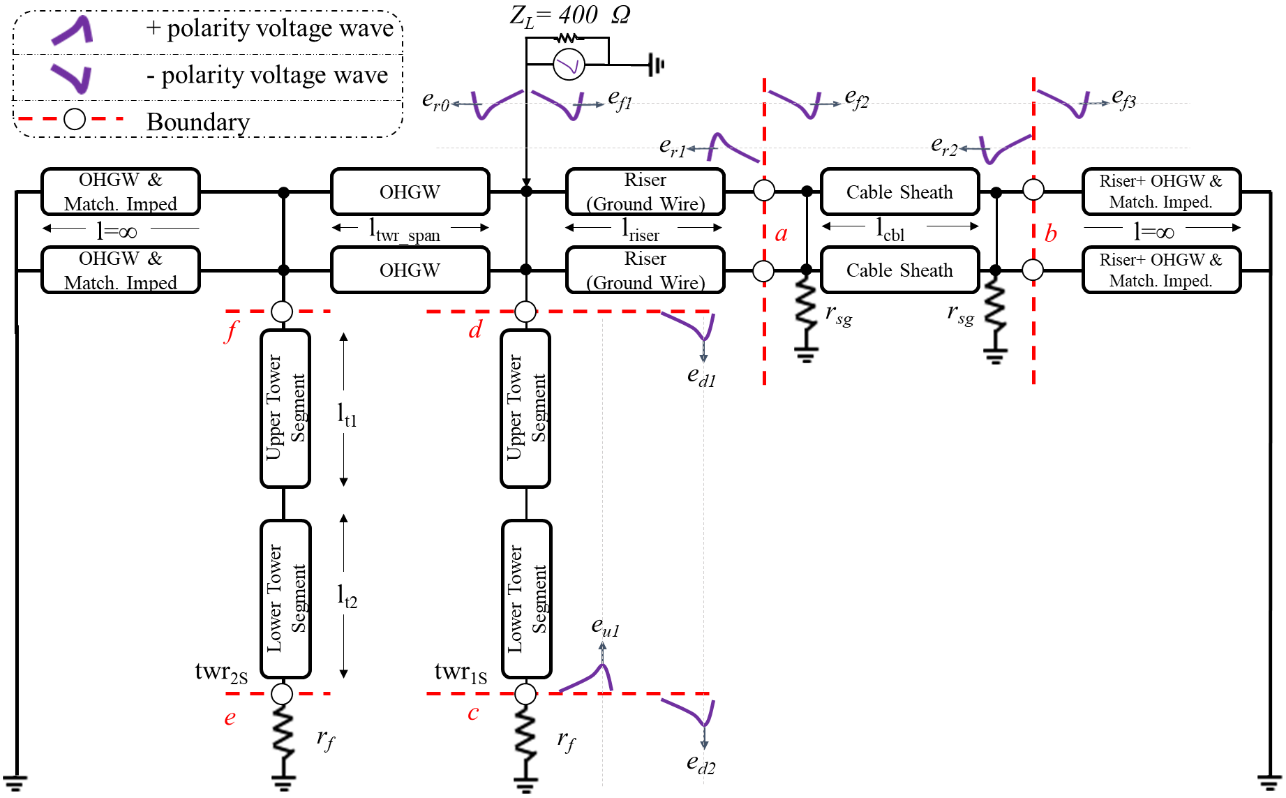

FIGURE 12. Equivalent circuit of mixed dc transmission line for analysis of indirect lightning strike on the tower top (only the two towers closest to the sending end of cable are considered in this equivalent circuit).

Therefore, attenuation of voltage on the tower top is caused by the reflected wave from the tower as well as from the cable sheath.

1) SHEATH-GROUND OVERVOLTAGE

Sheath-ground overvoltage (V_{SG}) stresses the outer insulation layer of the cable and can cause breakdown of the dielectric.

Firstly, the sheath of a 25 km cable is grounded only at the terminals. V_{SG} at various locations along the cable when lightning strikes at transition tower (twr_{1S}) is shown in Fig. 13. Lightning overvoltage is the highest at the cable entrance and it is attenuated to a very low value at the receiving end of the cable. This can be attributed to the large attenuation constant of the cable sheath.

To study the effect of the sheath grounding distance, a 25 km cable is divided into several segments, each grounded at its terminals. V_{SG} at various locations in the cable when lightning strikes twr_{1S} is shown in Fig. 14. The peak overvoltage at the cable entrance is unaffected by grounding the sheath at intermediate locations in the cable. However,

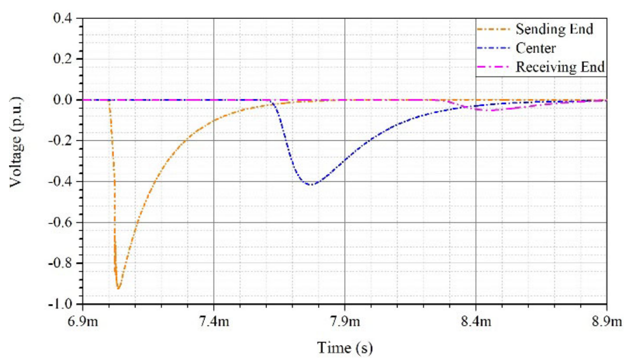

FIGURE 13. Lightning strikes the top of sending end transition tower (twr_{1S}). Sheath to ground voltage in a 25 km cable with sheath grounded at terminals only (r_{sg}=10 Ω).

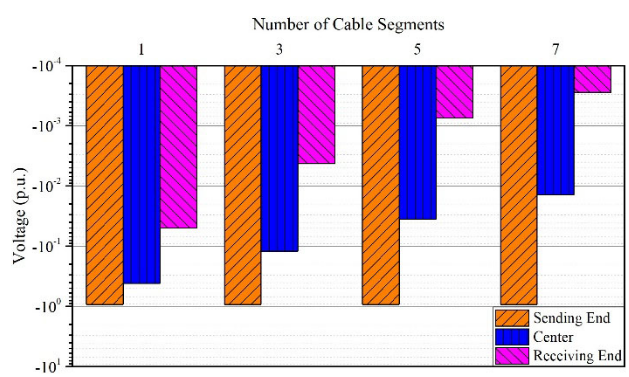

FIGURE 14. Sheath-ground voltage in a 25 km cable as a result of lightning strike on the top of sending end transition tower (twr_{1S}). Cable is divided into number of segments and each segment is grounded at the terminals.

the peak magnitude of V_{SG} inside the cable and at the far end decreases. The peak overvoltage decreases by decreasing the sheath grounding impedance, as shown in Fig. 15. Also, the peak voltage decreases significantly if lightning strikes farther away from the cable, as shown in Fig. 16. This is due to absorption of part of the voltage surge by intermediate towers between the cable and the location of the strike.

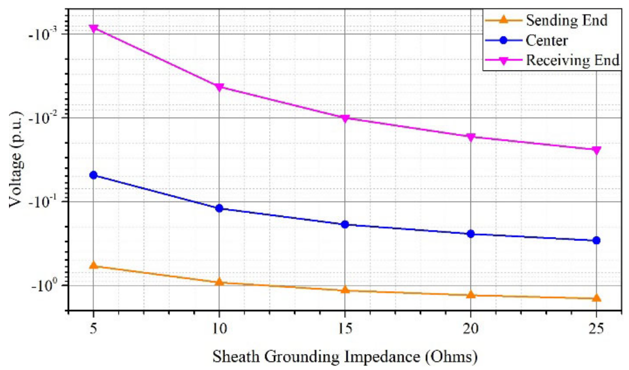

FIGURE 15. Sheath-ground voltage in a cable with variable sheath grounding resistance (r_{sg}). Sheath is grounded at terminals only.

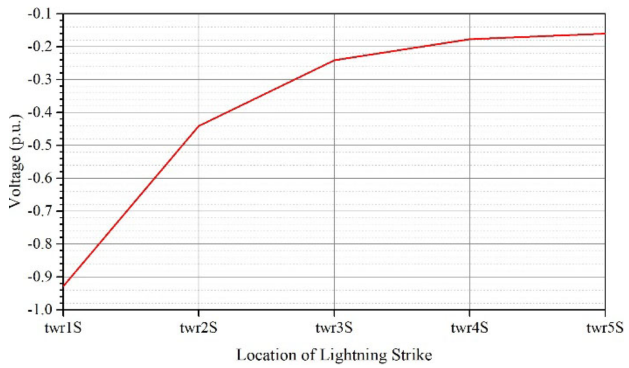

FIGURE 16. Sheath to ground voltage at the sending end of a 25 km cable for tower top lightning strikes at various locations.

2) OVERVOLTAGE STRESS ON INSULATORS

Tower top lightning strikes causes buildup of voltage on tower and overvoltage across insulators which may result in insulator flashover. The magnitude of the peak overvoltage across the +pole and −pole insulators because of tower top lightning strikes is shown in Fig. 17.

In the case of negative polarity lightning strikes, the voltage across + pole insulator will always be higher than the negative pole insulator. Therefore, + pole insulators will be more prone to flashover.

Flashover is possible only on + pole insulator of twr_{2S}. It can be seen in Fig. 18 that the rapid leader growth of the + pole insulator of twr_{2S} takes place at about 7.0248 and 7.0278 ms, respectively. This corresponds to the time of arrival of the peak of the reflected wave from the base of the adjacent towers i.e., twr_{1S} and twr_{3S}.

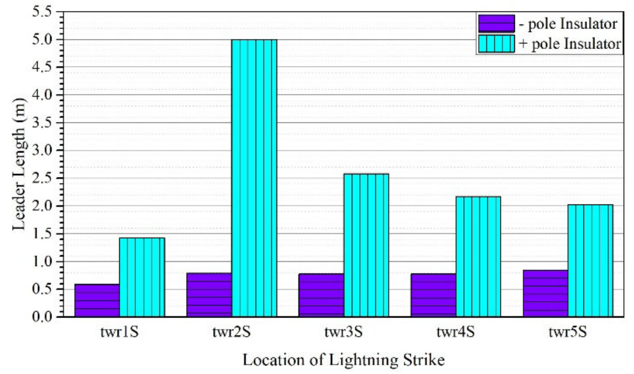

FIGURE 17. Leader growth between insulator arc horns resulting from lightning strikes on the top of respective towers.

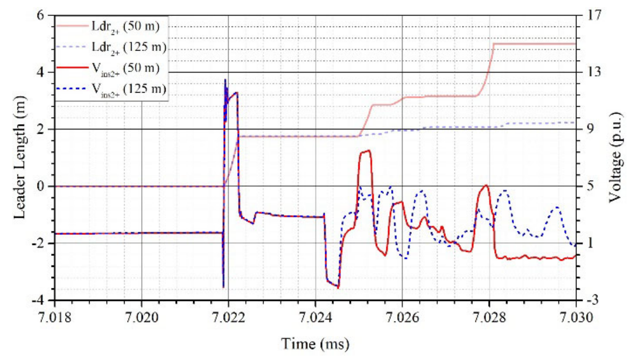

FIGURE 18. Influence of length of riser section (l_{riser}) on flashover performance of plus pole insulator of sending end subsequent tower (twr_{2S}).

However, when the length of the riser section is 50 m, the reflected wave from the sheath also arrives at the same time and superimposes with the reflected waves from the adjacent towers, resulting in accelerated leader growth and eventual flashover of the insulator. However, for 125 m long riser sections, the part of reflected wave from the sheath will be sufficiently delayed and the leader growth will stop.

The higher footing impedance increases the vulnerability of insulator flashover as shown in Fig. 19. The higher footing impedance results in a decrease in the positive polarity volt-

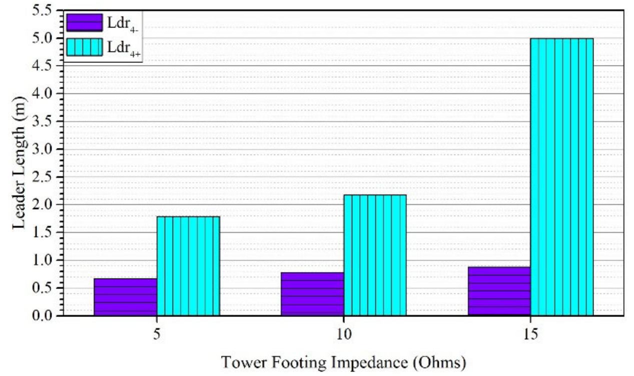

FIGURE 19. Influence of tower footing impedance on leader growth. Lightning strikes on top of twr_{4S}.

age surge reflected from the tower base. Therefore, the voltage stress across insulators will be higher and so will their vulnerability to flashover.

V. CONCLUSION

Lightning strikes are possible on overhead sections of mixed transmission lines. Overvoltage is produced in the transmission line due to lightning strikes which can stress the insulation of the overhead line as well as the cable. Excessive stress on the OHL insulator can cause flashover, which appears as a ground fault on the transmission line. On the other hand, excessive overvoltage stress on a cable can cause permanent failure of its insulation.

The following issues, which were previously unstudied or identified as important research questions, have been addressed in this paper.

1- Towers adjacent to cables are highly resistant to insulator flashover due to the quick arrival of opposite polarity reflected voltage surge from the cable.

2- Longer riser sections increase the vulnerability of OHL insulators to flashover.

3- A direct lightning strike on the OHGW or tower top can cause back flashover of insulators.

   a. Back flashover of positive polarity insulators is more likely.

   b. Under the conditions of our study, back flashover is most likely to occur on the twr_{2S}. However, this vulnerability can be alleviated by increasing the length of the riser section.

   c. Higher tower footing impedance increase the likeliness of insulator flashover.

4- A direct lightning strike on the OHGW or tower top can cause sheath to ground overvoltage.

   a. Sheath to ground overvoltage will be more severe at the cable entrance and attenuates significantly inside the cable or at the farther end of the cable.

   b. Sheath to ground overvoltage decreases with a decreasing sheath grounding impedance.

   c. Sheath to ground overvoltage inside the cable, or at the farther end of the cable, decreases slightly by decreasing the sheath grounding distance. However, sheath to ground overvoltage at the cable entrance is not affected by the sheath grounding distance.

Modeling guidelines as well as past literature has not emphasized the importance of riser sections on the transient performance of mixed transmission lines. Considering its significance, it is important to devise accurate electromagnetic models of riser sections based on the physical phenomenon.

REFERENCES

[1] D. Jovcic and K. Ahmed, "Introduction to line commutated HVDC," in *High Voltage Direct-Current Transmission Converters, Systems and DC Grids*, 2nd ed. West Sussex, U.K.: Wiley, 2015, ch. 1, sec. 1.1, pp. 1–3.

[2] N. M. Kirby, L. Xu, M. Luckett, and W. Siepmann, "HVDC transmission for large offshore wind farms," *Power Eng. J.*, vol. 16, no. 3, pp. 135–141, Jun. 2002.

[3] Q. Bui-Van, G. Beaulieu, H. Huynh, and R. Rosenqvist, "Overvoltage studies for the St. Lawrence river 500-kV DC cable crossing," *IEEE Trans. Power Del.*, vol. 6, no. 3, pp. 1205–1213, Jul. 1991.

[4] F. F. Silva, K. S. Pedersen, and C. L. Bak, "Lightning in hybrid cable overhead lines and consequent transient overvoltages," in *Proc. IPST*, Seoul, South Korea, 2017, pp. 1–7.

[5] A. F. Imece *et al.*, "Modeling guidelines for fast front transients," *IEEE Trans. Power Del.*, vol. 11, no. 1, pp. 493–506, Jan. 1996.

[6] T. Henriksen, "Calculation of lightning overvoltages using EMTP," in *Proc. IPST*, Lisbon, Portugal, 1995, pp. 1–5.

[7] *Recommendations for Testing DC Extruded Cable Systems for Power Transmission at a Rated Voltage up to 500 kV*, document CIGRÉ Brochure 496, CIGRÉ, WG B1.32, Apr. 2012.

[8] IEC Standard 62067, Ed.2.0, Nov. 2011. "Power Cables With Extruded Insulation and Their Accessories for Rated Voltages Above 150 kV (U_m =170 kV) up to 500 kV (U_m =550 kV)—Test Methods and Requirements."

[9] L. Colla, F. M. Gatta, A. Geri, and S. Lauria, "Lightning overvoltages in HV-EHV 'mixed' overhead-cable lines," in *Proc. IPST*, Lyon, France, 2007, pp. 1–6.

[10] F. Massaro, G. Morana, and R. Musca, "Transient behaviour of a 'mixed' overhead-cable EHV line under lightning events," in *Proc. UPEC*, Glasgow, U.K., Sep. 2009, pp. 1–5.

[11] G. Hoogendorp, M. Popov, and L. van der Sluis, "Lightning induced overvoltages in mixed 380 kV OHL-cable-OHL connections," in *Proc. IPST*, Vancouver, BC, Canada, 2013, pp. 1–6.

[12] M. Goertz *et al.*, "Lightning overvoltages in a HVDC transmission system comprising mixed overhead-cable lines," in *Proc. IPST*, Seoul, South Korea, 2017, pp. 1–6.

[13] M. Kizilcay and C. Neumann, "Lightning overvoltage analysis of a 380 kV overhead line with a GIL section," in *Proc. IPST*, Cavtat, Corotia, 2015, pp. 1–6.

[14] A. Ametani and T. Kawamura, "A method of a lightning surge analysis recommended in Japan using EMTP," *IEEE Trans. Power Del.*, vol. 20, no. 2, pp. 867–875, Apr. 2005.

[15] A. Ametani, N. Nagaoka, T. Ohno, and Y. Baba, "Transient on overhead lines," in *Power System Transients: Theory and Applications*, vol. 4, 2nd ed. Boca Raton, FL, USA: CRC Press, 2017, ch. 2, sec. 2, pp. 176–193.

[16] M. Ishii *et al.*, "Multistory transmission tower model for lightning surge analysis," *IEEE Trans. Power Del.*, vol. 6, no. 3, pp. 1327–1335, Jul. 1991.

[17] W. A. Chisholm, "New challenges in lightning impulse flashover modeling of air gaps and insulators," *IEEE Elect. Insul. Mag.*, vol. 26, no. 2, pp. 14–25, Mar./Apr. 2010.

[18] E. Stern *et al.*, "The Neptune regional transmission system 500 kV HVDC project," in *Proc. CIGRE*, Paris, France, 2008, pp. 1–8.

[19] L. V. Bewley, *Traveling Waves on Transmission Systems*. New York, NY, USA: Dover, 1963.

[20] A. Soares, M. A. O. Schroeder, and S. Visacro, "Transient voltages in transmission lines caused by direct lightning strikes," *IEEE Trans. Power Del.*, vol. 20, no. 2, pp. 1447–1452, Apr. 2005.

[21] *Guide to Procedures for Estimating the Lightning Performance of Transmission Lines*, document CIGRÉ Tech. Brochure 63, CIGRÉ Working Group 33.01, 1991.

[22] *IEEE Guide for Improving the Lightning Performance of Transmission Lines*, IEEE Standard 1243-1997, 1997.

[23] R. B. Anderson and A. J. Eriksson, "Lightning parameters for engineering application," *Electra*, vol. 69-4, p. 65102, Mar. 1980.

[24] G. Mazzanti and M. Marzinotto, "Improved design of HVDC extruded cable systems," in *Extruded Cables for High-Voltage Direct-Current Transmission: Advances in Research and Development*, vol. 8, 1st ed. Hoboken, NJ, USA: Wiley, 2013, ch. 5, sec. 5, pp. 251–252.

[25] L. Trim, B. Gregory, and D. Notman, "DC cable systems with extruded dielectrics," EPRI, Palo Alto, CA, USA, Tech. Rep. 1008720, Dec. 2004.

[26] T. V. Gomes, M. A. O. Schroeder, R. Alipio, A. C. S. de Lima, and A. Piantini, "Investigation of overvoltages in HV underground sections caused by direct strokes considering the frequency-dependent characteristics of grounding," *IEEE Trans. Electromagn. Compat.*, vol. 60, no. 6, pp. 2002–2010, Dec. 2018.

[27] M. Goertz, S. Wenig, C. Hirsching, M. Kahl, M. Suriyah, and T. Leibfried, "Analysis of extruded HVDC cable systems exposed to lightning strokes," *IEEE Trans. Power Del.*, vol. 33, no. 6, pp. 3009–3018, Dec. 2018.

[28] M. Marzinotto, G. Mazzanti, and C. Mazzetti, "A deeper insight into impulse levels selection for long DC extruded cable lines," in *Proc. Annu. Rep. Conf. Electr. Insul. Dielectric Phenomena*, Montreal, QC, Canada, 2012, pp. 387–390.

[29] *Overvoltages on HVDC Cables Final Report*, document CIGRÉ Brochure 86, CIGRÉ JWG 33/21/14.16, 1994.

[30] T. Ito, T. Ueda, H. Watanabe, T. Funabashi, and A. Ametani, "Lightning flashovers on 77-kV systems: Observed voltage bias effects and analysis," *IEEE Trans. Power Del.*, vol. 18, no. 2, pp. 545–550, Apr. 2003.

[31] Z. G. Datsios and P. N. Mikropoulos, "Effect of tower modelling on the minimum backflashover current of overhead transmission lines," in *Proc. 19th Int. Symp. HV Eng.*, Pilsen, Czech Republic, 2015.

[32] J. A. Martinez and F. Castro-Aranda, "Tower modeling for lightning analysis of overhead transmission lines," in *Proc. IEEE Power Eng. Soc. General Meeting*, San Francisco, CA, USA, Jun. 2005, pp. 1212–1217.

[33] I. S. Grant *et al.*, "A simplied method for estimating lightning performance of transmission lines," *IEEE Trans. Power App. Syst.*, vol. PAS-104, no. 4, pp. 919–932, Jul. 1985.

[34] W. A. Chisholm, Y. L. Chow, and K. D. Srivastava, "Travel time of transmission towers," *IEEE Trans. Power App. Syst.*, vol. PAS-104, no. 10, pp. 2922–2928, Oct. 1985.

[35] R. Alipio and S. Visacro, "Frequency dependence of soil parameters: Effect on the lightning response of grounding electrodes," *IEEE Trans. Electromagn. Compat.*, vol. 55, no. 1, pp. 132–139, Feb. 2013.

[36] D. Cavka, N. Mora, and F. Rachidi, "A comparison of frequency-dependent soil models: Application to the analysis of grounding systems," *IEEE Trans. Electromagn. Compat.*, vol. 56, no. 1, pp. 177–187, Feb. 2014.

[37] IEC Standard TR 60071–4, 1st ed., Apr. 2004. "Insulation co-ordination—Part 4: Computational guide to insulation co-ordination and modelling of electrical networks."

[38] A. Morched, B. Gustavsen, and M. Tartibi, "A universal model for accurate calculation of electromagnetic transients on overhead lines and underground cables," *IEEE Trans. Power Del.*, vol. 14, no. 3, pp. 1032–1038, Jul. 1999.

[39] B. Gustavsen, G. Irwin, R. Mangelrød, D. Brandt, and K. Kent, "Transmission line models for the simulation of interaction phenomena between parallel AC and DC overhead lines," in *Proc. IPST*, Budapest, Hundary, 1999, pp. 61–67.

[40] P. Chowdhuri *et al.*, "Parameters of lightning strokes: A review," *IEEE Trans. Power Del.*, vol. 20, no. 1, pp. 346–358, Jan. 2005.

[41] P. N. Mikropoulos and T. E. Tsovilis, "Lightning attachment models and maximum shielding failure current of overhead transmission lines: Implications in insulation coordination of substations," *IET Gener. Transmiss. Distrib.*, vol. 4, no. 12, pp. 1299–1313, 2010.

MANSOOR ASIF (S'15) was born in Pakistan, in 1991. He received the bachelor's degree in electrical engineering from the National University of Sciences and Technology (NUST), Pakistan, in 2013, and the master's degree in electric power systems from the North China Electric Power University, Beijing, in 2015.

He is currently pursuing the Ph.D. degree with the HVDC Electric Power Lab, Hanyang University, Ansan, South Korea. He was a Lecturer with the School of Electrical Engineering and Computer Science, NUST, Pakistan, where he was involved in teaching at the bachelor's level. His current research interests include overvoltage analysis and insulation coordination studies for dc grids.

Mr. Asif is a Student Member of CIGRE and a member of the Pakistan Engineering Council and the Korean Institute of Electrical Engineers.

HO-YUN LEE (S'15) was born in Seoul, South Korea, in 1987. He received the bachelor's degree in electronic system engineering from Hanyang University, Ansan, South Korea, in 2014.

He is currently pursuing the combined M.S.–Ph.D. degrees with the HVDC Electric Power Lab, Hanyang University. His current research interests include power system analysis and protection equipment for dc grids.

Mr. Lee is a Student Member of CIGRE and the Korean Institute of Electrical Engineers.

UMER AMIR KHAN (M'10) was born in Karachi, Pakistan, in 1984. He received the B.E. degree in electronics engineering from the National University of Sciences and Technology (NUST), Islamabad, Pakistan, in 2006, and the M.S. and Ph.D. degrees from Hanyang University, Ansan, South Korea, in 2011 and 2016, respectively.

He was an Assistant Professor with NUST, Pakistan, until 2016. Since 2016, he has been an Assistant Professor with the Capital University of Science and Technology, Pakistan. His research interests include protection systems and switchgear design for HVDC systems, high-voltage power electronics, motor drives, photovoltaics, and the design of training and laboratory equipment.

Dr. Khan is a Registered Engineer with the Pakistan Engineering Council and a member of KIEE and the IEEE Power and Energy Society.

KYU-HOON PARK (S'16) was born in Seoul, South Korea, in 1991. He received the bachelor's degree in electronic system engineering from Hanyang University, Ansan, South Korea, in 2016.

He is currently pursuing the combined M.S.–Ph.D. degree with the HVDC Electric Power Lab, Hanyang University. His current research interests include power system analysis and protection equipment for dc grids.

Mr. Park is a Student Member of CIGRE and the Korean Institute of Electrical Engineers.

BANG-WOOK LEE (M'10) was born in Jeju, South Korea, in 1968. He received the bachelor's, master's, and Ph.D. degrees from Hanyang University, Seoul, South Korea, in 1991, 1993, and 1998, respectively, all in electrical engineering.

He was a Senior Research Engineer with LS Industrial Systems Co., Ltd., South Korea. In 2008, he joined the Department of Electronic System Engineering, Hanyang University, Ansan, South Korea, where he is currently a Professor. His research interests include high voltage insulation design, high-voltage dc (HVDC) protection systems, and the development of electrical equipment including transmission line structures for HVDC and HVAC power systems.

Dr. Lee is the Scholar Director and a member of the HVDC Research Committee of the KIEE and a member of the Power Cable Experts Committee of the Korean Agency for Technology and Standards and CIGRE.